



Experimental Investigation of Porosity, Installation Angle, Thickness and Second Layer of Permeable Obstacles on Density Current

A. Jahangir^a, K. Esmaili^{*a}, M. F. Maghrebi^b

^a Department of Water science and Engineering, Ferdowsi University of Mashhad, Mashhad, Iran

^b Department of Civil Engineering, Ferdowsi University of Mashhad, Mashhad, Iran

PAPER INFO

Paper history:

Received 07 March 2020

Received in revised form 26 April 2020

Accepted 25 July 2020

Keywords:

Density Current

Obstacle Porosity

Obstacle Installation Angle

Obstacle Thickness

Second Layer of Obstacle

Permeable Obstacle

ABSTRACT

This study explored the effect of porosity and installation angle, thickness (dimension) and second layer of permeable obstacles on density current control and trapping in the laboratory. For this purpose, an insoluble suspended polymer and two types of groove and cavity obstacles made from plexiglass sheets were selected. The experiments were conducted with two different concentrations, five different porosities, four different angles, four different thicknesses and two obstacle layers. The results showed that the optimum porosities for cavity and groove obstacles were 22 and 19%, respectively. In all experiments, the cavity trapping rates of 0.13% and 0.14% at 10% and 20% concentrations were higher than those of groove trapping. In addition, by increasing the angle, the rate of trapping decreased and its value was observed in the groove with the correlation coefficients of 0.995 and 0.981 compared to the cavity. The major effect of obstacles was found to be the flow deceleration where the average velocity in the cavity was obtained 3.62% higher than that in the groove. For the increased thickness with 10% porosity and groove type, the passage of materials from the obstacle further increased. By creating the second layer of obstacle, the passage of materials from the obstacle in the both groove and cavity increased, and the optimal distance of the second obstacle was 2.25 m from the first one.

doi: 10.5829/ije.2020.33.09c.03

1. INTRODUCTION

The mechanism of flow sedimentation are among the important and complex issues in hydraulic structures; the issue has been paid attention by many experts [1-4]. Sediments can have significant effect on the behavior of a density current [5]. Density current occurs when a fluid of high density flows into a low density or light fluid [6-8]. One of the effective tools to control flow sediment is the obstacles used in the river course upstream of main structures and dam reservoirs [9, 10]. Permeable obstacles are more common and efficient due to the ability to pass part of the flow and reduce the flow pressure compared to impermeable obstacles [11, 12]. Since the major part of sediments is related to the suspended load of flow, which occurs in the floods and density currents, it is very important to understand and study these types of currents. De Cesare et al. [13]

evaluated the passage of density current through different obstacles. Their studies showed that the density current can be effectively designed through the constructive measurements. Asghari Pari et al. [14] presented the velocity curves of flow body and concentration. They concluded that the high height is more effective on the flow control and also at high concentrations, the effect on the velocity and control of flow sediment is also high. Oehy and Schleiss [15] investigated the effect of different obstacles on the control of density current and concluded that the subcritical conditions and not passing over the obstacle are more appropriate. To compare experimentally the effect of porous obstacle and porous stepped obstacle on the control of density current, Kordnaeij et al. [16] used porous obstacle as a permeable ones. The results of the study showed that the porous obstacle outperforms the porous stepped obstacle and further reduces the sediment discharge. Asghari Pari et

*Corresponding Author Institutional Email: esmaili@um.ac.ir (K. Esmaili)

al. [17, 18] numerically investigated the effect of the angle upstream the obstacle and depth of water reservoir on controlling the density current. They stated the high the obstacle height, the low impact of water depth would better control the flow. In addition, the high angle upstream of obstacle would be the greater the flow control by obstacle. Habib Mohammadi et al. [19] studied the effect of height, shape and location of gabion obstacles on the control of sediment density current. They stated that part of the flow passes through or over the obstacle and the high height and close to the inlet, the low velocity resulted in desired performance. Alves and Rossato [20] conducted a series of experiments to investigate the effect of obstacles on density currents. The results showed that the flow velocity decreases with an increase in the obstacle height; while the ratio of different characteristics remains constant in the velocity profile. In a study conducted by Nogueira et al. [21], the dynamic properties of density current on rough bed in experiment approaches were evaluated. The convergence of upstream Froude number showed that the mechanical characteristics of the flow were determined by the means of upstream local variables. Janocko et al. [22] found that the superiority of numerical simulations is the possibility of monitoring all the hydraulic factors in the density current and their reactions to the three-dimensional topography of the walls during the full flow period. In another study, MacArthur et al. [23] experimentally analyzed the density currents using the imaging technique. They concluded that the obstacles with uneven surface reduce the flow velocity, but have a slight effect on the overall flow velocity. Yaghubi et al. [24] experimentally investigated the effect of inlet concentration on the flow behavior in the presence of two consecutive obstacles. The study results showed that an area with an insignificant velocity and significant concentration grows at the top of each obstacle and with the increased inlet concentration, the area becomes larger. Zeinivand et al. [25] investigated the porosity percentage of obstacles and different flow concentrations. The results showed that by increasing the porosity percentage of the obstacles, the absorption rate of flow materials decreased and correspondingly, the efficiency of obstacles in the control of flow will be lower. Abhari et al. [26] examined the transfer rate of experimentally suspended load. This study showed that in the velocity profile, the obstacle reflects the flow and creates another critical area in addition to the walls in the current, reducing 1% of the average transfer rate of suspended load in downstream the obstacle.

Despite the numerous studies to understand the behavior of density currents [28-30], evaluating the behavior of currents with suspended sediment load colliding with permeable obstacles in their way is a novel issue. There was less report and still needs further investigation. For this purpose, as presented in Figure 1,

this paper explores the effect of porosity and installation angle, thickness (dimension) and second layer of permeable obstacles on the density current control and trapping in the laboratory.

2. MATERIALS AND METHODS

2. 1. Laboratory Equipment

In this study, a flume with the length of 10 m, width of 30 cm and height of 45 cm was used. Figure 2 shows the overall view of the flume and the related laboratory equipment. The study tests were conducted for duration of 6 months in the hydraulics and sediment laboratory of Water Engineering Department in Agriculture Faculty of Birjand University. Due to constant flow, the velocity recording, collision status and passage of flow over the obstacles were performed using the Pitot tube plate by the imaging technique. The Pitot tube plate was installed in the upstream of the obstacles with measuring capability at distance of 5 cm, and the imaging was performed solely to examine the density current motion along the flume; the physical and mechanical behavior of the collision and passage of flow over the obstacles. The longitudinal slope values were considered zero in the experiments. The plexiglass sheets of 3 mm thick with the width equal to the flume width and the height up to 30 cm were used to build the obstacles. The amount of porosity in the obstacles with different percentages of 10, 15, 20, 25 and 30 in both forms of groove and cavity were created using the equal groove width and diameter of 3 mm (about 3 times the average particle diameter). The obstacles were installed at the distance of 9 m from the inlet of density current injection. The obstacle installation angles were considered at 45, 60, 75 and 90° relative to the direction perpendicular to the bed. Figure 3 shows samples of two types of cavity and groove obstacles.

2. 2. Density Current Characteristics

The desired density current was produced by the mixture of

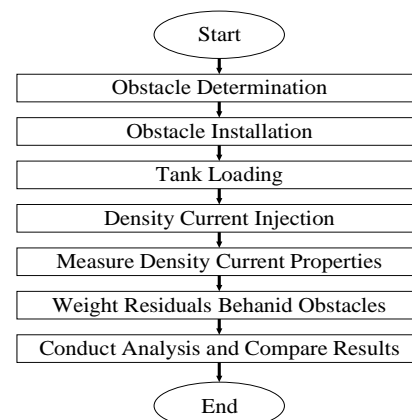


Figure 1. Overall paper flowchart

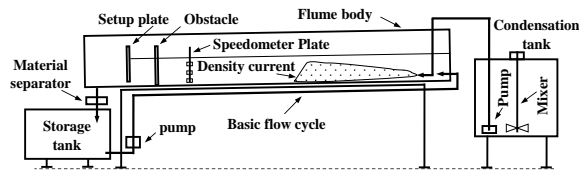


Figure 2. Overall view of flume and laboratory equipment

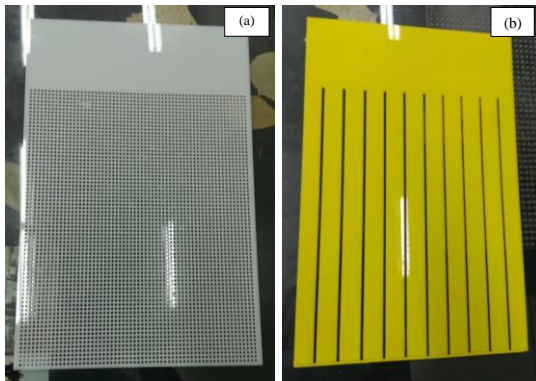


Figure 3. Samples of used obstacles: a) cavity obstacle; b) groove obstacle

water and a type of expanded poly styrene (EPS) with the density of 1135 kg/m^3 and average diameter of 1.15 mm. The current was injected into the main stream at an average discharge of 3.43 L/s at a distance of 7 cm from the bottom of the flume. The density current injection was performed by pump as flood hydrograph. The base water discharge was 5 L/s and the volume of density current was 460 L with a mixer at two different concentrations of 10 and 20%. At the end of the flume, there was a filter and a tank for separating materials from the current for the storage and reuse purposes. Figure 4 shows the tank for the production of density current and the filter for the separation of materials from the current.

According to Figure 4(b), in the test device, a suitable filter with a total flow capacity was placed at the flume



Figure 4. a) Density current production tank; b) material separating filter

outlet against the flow to separate suspended matter passing through the obstacles and to store material-free flow into the storage tanks and continued the flow cycle for the experiments. In addition, the collected materials were the basis for evaluating the performance of the obstacles and used for subsequent tests.

2. 3. Test Method

To ensure that the material used is suspended, special experiments were carried out based on the proposed theories and the experimental method of mixing and falling speed. Then, the concentration tank was filled with water and the required amount of material for the desired concentration was added and homogenized with the mixer. By installing the control valve and obstacle, the base discharge was set and adjusted to the threshold depth. According to the characteristics of the current and polymer material and considering the limitations of the laboratory flume dimensions according to Schneider method [19], the depth of 25 cm was calculated. Then, as shown in Figure 5, the density current was injected to the stream as flood hydrograph.

As shown in Figure 5, out of the total test time (335.4 seconds), 84 seconds (25%) is dedicated to be the upward trend, 49.8 seconds (15%) to the peak constant discharge, and 201.6 seconds (60%) to the downward trend. The average pumping time is about 133.8 seconds.

To determine the testing time and to validate the test, the control sample was taken as the temporal variations of the suspended sediment load for the desired depth. In this way, the least change of the sediment load was the basis for the time selection, which resulted in the hydrograph, as shown in Figure 4. In all experiments, the flow characteristics including the velocity, body height, injection time, front and tail arrival time of suspended materials to the obstacle, process of collision with and passage over obstacle, situation and location of sedimentation, amount of passed and trapped materials behind the obstacle were measured. The obstacle performance criterion was the amount of trapped materials (fraction of passed materials to total initial material). In this study, 68 independent tests including density currents at two concentrations and five porosities, and obstacles using two different shapes, numbers and thicknesses and four installation angles, were performed.

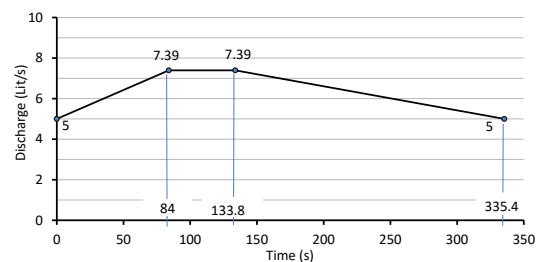


Figure 5. Flood flow hydrograph produced in experiments

3. RESULTS AND DISCUSSION

3. 1. Flow Velocity

The flow velocity measurement was performed with a piezometric plate attached to the pitot tubes and also using imaging of the flume sides. The velocity varied by the temporal variations of discharge, relative location of measurement and obstacle at different porosities. An example of the velocity profiles approaching the flow upstream of the obstacle is shown in Figure 6.

The reason for the relative increase in flow velocity in the vicinity of the obstacle can be attributed to the impact of the reduced passage over the obstacle and also the decrease in suspended sediment load along with upstream course. The vertical profiles of velocity and flow concentration at 2 and 5 m upstream of the obstacle are shown in Figure 7.

As can be seen in Figure 7, the density current approaches the obstacle, the average velocity is low and the depth velocity is more widely distributed. In addition, due to the sedimentation in the course to the obstacle, the concentration of materials decreases and the concentration in the deep sections of the stream increases. The depth changes in the vicinity of the upstream obstacles are shown in Figure 8. As can be seen in Figure 8, the high porosity, the low rate of depth decrease as the porosity increases. This trend was observed both for base flow without water level adjustment and for total flow with water level adjustment with depth. The upstream depth of the groove obstacles with an average of 4.14% is always higher than that of the cavity obstacles. The main reason for this difference was the desired distribution of cavities at the surface of cavity obstacle and the easier passage of flow through the cavities.

The studies showed that the velocity profiles differed along with flume depending on the position relative to the obstacle. As such, upstream of the obstacles, the velocities become more balanced with moving away from the obstacles and close to the form of flow without

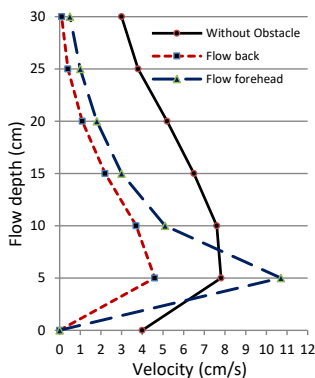


Figure 6. Example of velocity profiles approaching flow upstream of obstacle

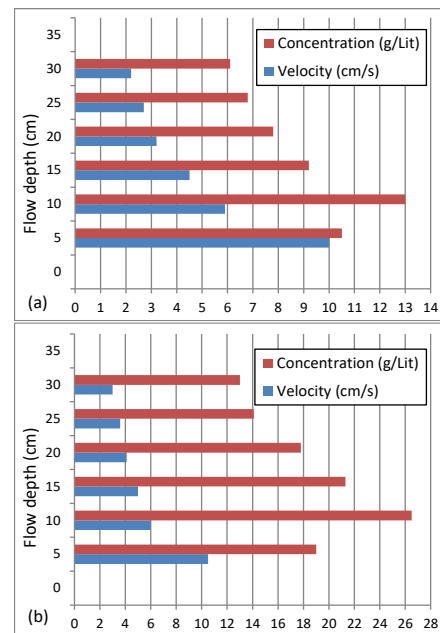


Figure 7. Vertical velocity profile and flow concentration with concentration of 20% in (a) 2m upstream of obstacle; (b) 5m upstream of obstacle

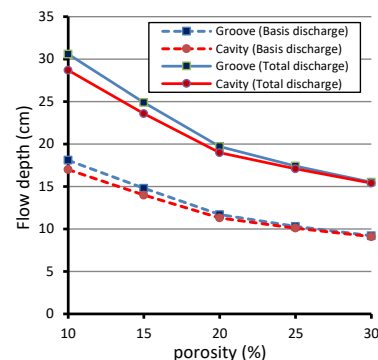


Figure 8. Depth changes in vicinity of obstacles for basis and total discharge

obstacle. In the vicinity of the obstacle, the velocities are more different in depth and higher than the maximum value. The currents with cavity obstacles had a lower upstream depth due to the easier flow while having 3.62% higher velocity. In addition, the mean velocity of the front and tail of density current mass were 10.7 and 4.6 cm/s, which were 37% higher and 30.2% lower than the mean flow velocity, respectively. The differences in velocities can be attributed to the obstacle performance in the flow deceleration and the trapping and sedimentation factors of the density current.

In addition to the velocity profiles and upstream depth, the test time was also evaluated. Figure 9 shows the test time from the beginning of the density current injection to the base flow until the passage of the last particle of suspended load over the obstacle.

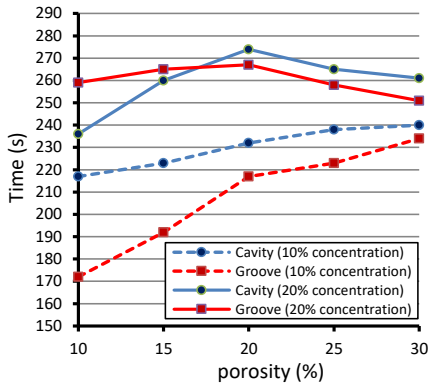


Figure 9. Variations of test time for obstacles with different flow concentrations

As shown in Figure 9, the distribution and temporal variations of the test time at concentration of 10% was greater than that of the 20% concentration. In addition, the variations of test time at the 20% concentration are more balanced compared to those of 10% concentration. The depth and flow velocity data in the vicinity of the upstream obstacles are summarized in Table 2.

The obtained results showed that as part of the flow passes through the obstacle body, the front velocity of the flow occurs with the same pattern as behind the obstacle. However, at high levels, the flow velocity is significantly reduced. It was also observed that the stationary state and even the inverse current of upper and surface parts caused by the collision of flow with obstacles is a factor behind the accumulation of part of the materials on the surface. It should be noted that since this part of the accumulated materials are not part of the suspended flow mass, the floating materials were deducted from the initial materials, which constitute about 11% of the total initial materials. Figure 10 shows how the sediments accumulate upstream of the obstacle.

3. 2. Effect of Obstacle Porosity To determine the effect of obstacle surface porosity with constant flow conditions, two types of obstacles were tested at two concentrations of 10 and 20% for five porosities of 10, 15, 20, 25 and 30%. Figure 11 shows the amount of



Figure 10. Accumulation of sediments upstream obstacle

materials passing over the obstacles versus the porosity. In addition, the related data are given in Table 3. By deducting the amount of passed material from the total initial material, the performance of the obstacle in trapping was determined and expressed in percent.

The results showed that in all cases, the trapping performance of the cavity obstacle is better than that of the groove obstacle, so that at concentrations of 10 and 20%, the average trapping of cavity obstacles was reported 0.14% and 0.13% higher than the groove obstacles, respectively. At low concentrations, the performance of the two types of obstacles is relatively similar, but at high concentrations, the cavity-type performance has been found to be more effective in

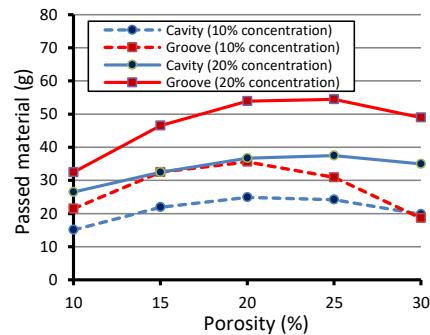


Figure 11. Variations of materials passing over obstacles with different porosities and concentrations

TABLE 2. Depth and flow velocity of upstream obstacles

| Porosity (%) | Depth (cm) | | Velocity (cm/s) | |
|--------------|------------|--------|-----------------|--------|
| | Groove | Cavity | Groove | Cavity |
| 10 | 9.2 | 9.8 | 30.6 | 28.7 |
| 15 | 11.3 | 11.9 | 24.9 | 23.6 |
| 20 | 14.3 | 14.8 | 19.7 | 19.0 |
| 25 | 16.2 | 16.5 | 17.4 | 17.1 |
| 30 | 18.1 | 18.3 | 15.5 | 15.4 |

TABLE 3. Material trapping data for different porosities and concentrations

| Porosity (%) | Material trapping (g) 10% concentration | | Material trapping (g) 20% concentration | |
|--------------|---|--------|---|---------|
| | Groove | Cavity | Groove | Cavity |
| 10 | 5010.1 | 5016.5 | 10030.6 | 10036.6 |
| 15 | 4999.1 | 5009.7 | 10016.6 | 10030.6 |
| 20 | 4996.0 | 5006.7 | 10009.2 | 10026.4 |
| 25 | 5000.7 | 5007.4 | 10008.6 | 10025.6 |
| 30 | 5013.0 | 5011.8 | 10014.1 | 10028.1 |

trapping materials. Also, at high porosity, the performance of the two types of obstacles was close together. In this case, the lowest trapping was observed in 20% porosity for 10% concentration and in 25% porosity for 20% concentration. By repeating the tests and further examining the optimal porosity, which has the highest amount of passed material, it was determined about 22% for the groove type and about 19% for the cavity type. The trapping decreases for the porosities lower than this amount and increases for the higher porosities.

3. 3. Effect of Obstacle Installation Angle In the first stage of tests, the obstacles were considered perpendicular to the flow direction (90° angle). To investigate the effect of the installation angle, the obstacles were rotated in the flow direction at the same previous location. According to Figure 12, the angles 90, 105, 120 and 135° were selected relative to the horizontal bed direction. The variations of the materials passing over the obstacles for different obstacle angles are shown in Figure 13. Table 4 also reports the data on the trapping performance for different obstacle installation angles (10% porosity) and different concentrations.



Figure 12. Selected angles of obstacle installation beyond 90°

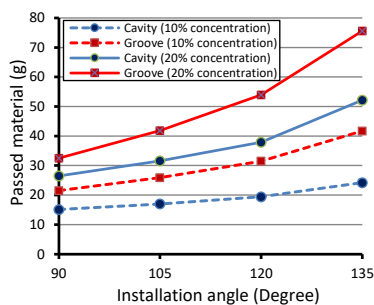


Figure 13. Variations of passed materials with obstacle installation angle at different concentrations

TABLE 4. Data on trapping performance for different obstacle installation angles (10% porosity) and concentrations

| Installation Angle (Dgree) | Material trapping (g) | | Material trapping (g) | |
|----------------------------|-----------------------|-------------------|-----------------------|---------|
| | 10% concentration | 20% concentration | Groove | Cavity |
| 90 | 5005.7 | 5016.5 | 10030.6 | 10036.6 |
| 105 | 5000.1 | 5014.6 | 10021.3 | 10031.6 |
| 120 | 4989.9 | 5012.2 | 10009.2 | 10025.2 |
| 135 | 5031.6 | 5007.4 | 9987.5 | 10010.9 |

The results showed that by increasing the angle of installation reduces the trapping level in both types of obstacle. In addition, at two different concentrations used, the observed reduction in the trapping level in the groove obstacles was more than that in the cavity obstacles. According to Figure 14, the correlation coefficients in the groove and cavity obstacles were 0.9994 and 0.9967 for 10% and 20% of concentration, respectively. This can be attributed to the easier passage of flow and discharge of materials due to the water pressure on the cavity obstacle. For this reason, the trapping reduction rate in the groove obstacles was more than that in the cavity obstacles.

3. 4. Effect of Obstacle Thickness or Dimension

To investigate the effect of obstacle thickness and dimension in the flow direction, one of the groove obstacles with 10% porosity was selected. Due to the operational limitations, according to Figure 15, this obstacle was used at a 90° angle in perpendicular direction. The passed current was constant with the same base current at both 10 and 20% concentrations. In addition to the thickness of the main obstacle (3 mm), the 5, 10 and 15cm thicknesses were also considered.

Figure 16 shows the amount of passed sediment for different obstacle thicknesses in both currents at 10 and 20% concentrations. As can be seen in Figure 16, the

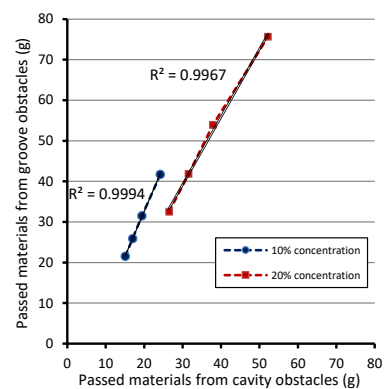


Figure 14. Relative fitting of materials passed over obstacles with different installation angles and concentrations



Figure 15. Example of obstacle with dimension for testing impact of obstacle thickness

amount of passed materials is higher for the increased obstacle thickness at both concentrations. However, at high concentration resulted in high increased rate. As such, the slope of fitting line of the 20% concentration data was observed about 2.3 times that of the 10% concentration. Also, the correlations of recorded data of the obstacle-passed materials with different thicknesses at the 10 and 20% concentrations were 0.981 and 0.995, respectively. The reason for the general increase in the passed materials was found to be the impact of the current passing along the obstacle on the current flowing into the obstacle and created suction conditions. Also, the higher correlation coefficient at higher concentration was attributed to the easier flow of suspended materials into the obstacle due to the inside flow tension. In the case of obstacles with low thickness, the flow is released as it passes over and has no effect on the upstream and, as a result, on the flow of materials through and over the obstacle.

3. 5. Effect of Second Obstacle Layer Due to the frequent application of sediment control structures such as slit dams, an obstacle was used to investigate the effect

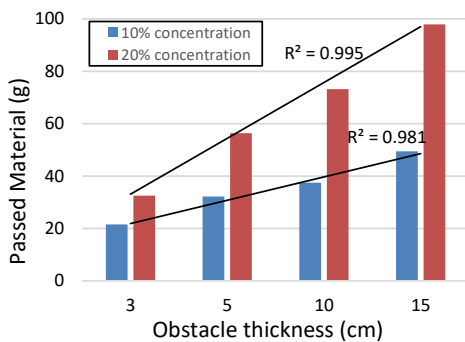


Figure 16. Amount of passed sediment for different thicknesses of first obstacle with two rows and 10 and 20% concentrations

of the second obstacle upstream of the main one. The tests were performed for all previously used obstacles with the same specifications but with a half-height obstacle. The relevant experiments were repeated at the same conditions as before with two concentrations of 10 and 20% and the materials deposited behind an obstacle and the conditions of two obstacles were compared. Figure 17 illustrates the second-layer obstacle and the obstacle valve for the passage of second-layer materials. A view of the deposited material with the second layer of obstacle is shown in Figure 18.

The amount of sediment passed over a single obstacle, two obstacles, comparison of the obstacle types in two obstacles, and the remaining amount behind the second obstacle are shown in Figures 19, 20, 21 and 22, respectively.

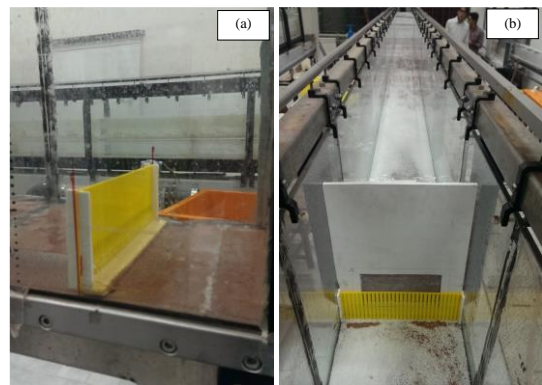


Figure 17. a) Example of second-layer obstacle; b) valve for passage of second-layer

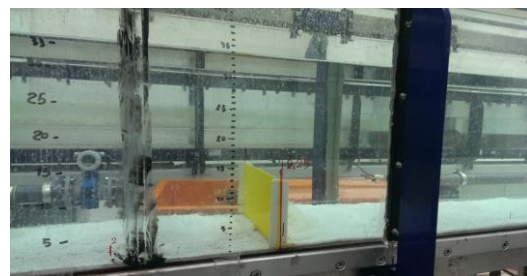


Figure 18. View of deposited material with second layer of obstacle

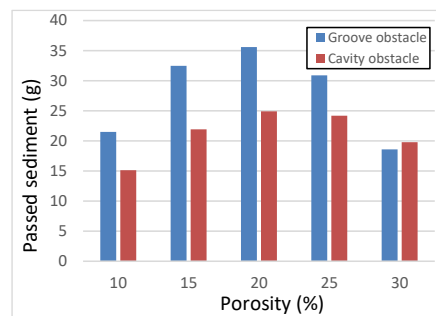


Figure 19. Amount of sediments passed over single obstacle

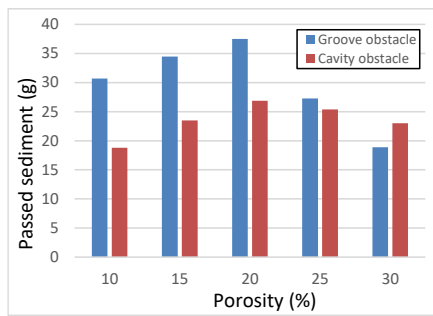


Figure 20. Amount of sediments passed over two obstacles

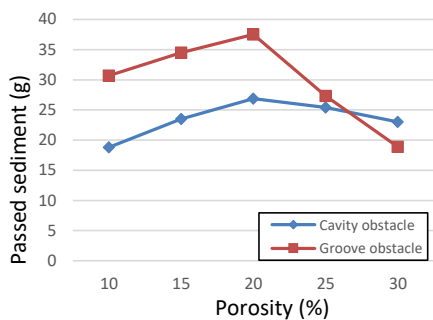


Figure 21. Comparison of sediment amounts passed over first obstacle in case of two obstacle rows

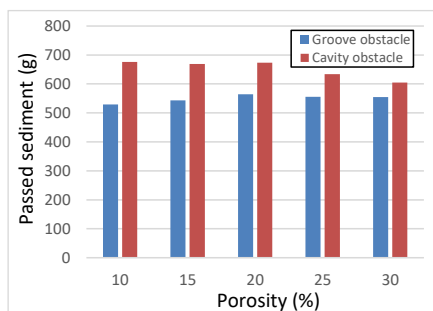


Figure 22. Amount of sediment remained behind second obstacle

As shown in Figures 19 and 20, by addition of the second layer of obstacle, the amount of passage over the first layer slightly increased compared to the single-obstacle conditions. The average amounts of increased for the cavity and groove obstacles were 2.34% and 1.96%, respectively. The reason for such increase was the effect of turbulent flow passing over the second obstacle towards the first obstacle downstream and the tendency of the materials to the passage. The behavior of groove and cavity obstacles was similar to the single-layer case. As such, the optimal porosity in this case was also observed about 20% where the passage of materials over the obstacle before and after that had an increasing and decreasing trend, respectively. In this case, the efficiency

of the cavity-type obstacle was better than the groove type.

Comparing the behavior of the two types of cavity and groove obstacles in Figure 21 showed that by addition of the second obstacle row, the materials passing over the first obstacle downstream in the cavity type had less changes than the groove type. Particularly for the porosities higher than the optimum porosity (about 20%), the groove-type conditions were improved so that at high porosities, the efficiency was higher than the cavity type. This is due to low permeability of the obstacle than the cavity type resulted from the flow turbulence.

The examination of the materials deposited behind the second obstacle in Figure 22 showed that with an increasing the porosity before the optimum porosity, the trapping process decreased, but that of the groove type increased. For the porosity more than the optimal porosity, due to high permeability of the cavity type, the same process was continued, but in the groove type, as the flow passes over obstacle, the trapping and sedimentation of materials behind the obstacle were stabilized. However, the performance of both types of obstacle showed that the second layer was effective in improving the obstacle efficiency. Of course, it was affected by the distance of the second obstacle from the first obstacle.

To investigate the effect of location and installation of second obstacle to the first one, the experiments were carried out from 2 m upstream the first obstacle at 25cm intervals to the end of flume. The reason for choosing 2 m was that in the lower distances, the turbulence of the flow passing over the second obstacle had a great effect on the first obstacle and the performance of obstacles could not be distinguished. As such, for the performed experiments, the optimal distance of the second obstacle from the first one downstream was determined based on the highest trapping and sedimentation efficiencies. The selection criterion was to compare the deposited materials between the two obstacles and upstream of the second obstacle layer. Figures 23 and 24 showed the amount of the sediment passed over the first and second obstacle in terms of the distance from the first obstacle, respectively.

The studies showed that the greater the distance between the second and first obstacles, the better the effectiveness in improving the efficiency. Figure 24 shows that the process of sediment deposition behind the second obstacle is greater with an increased distance from the first obstacle. Also, according to Figure 23, it was found that with the existing tools and limitations, the sedimentation process changed from a certain distance to higher ones. The reason for this was also the effect of turbulence caused by the base flow inlet, especially the effect density current injection. As a result, at the end parts of the flume, the function of the second layer was

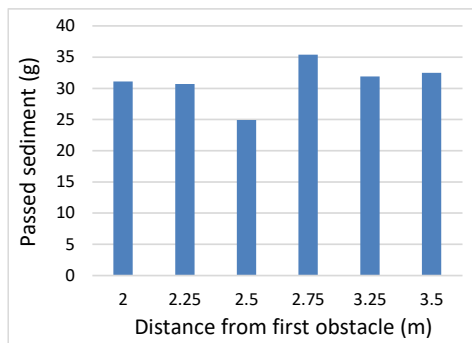


Figure 23. Amount of sediment passed over first obstacle in terms of distance from first obstacle

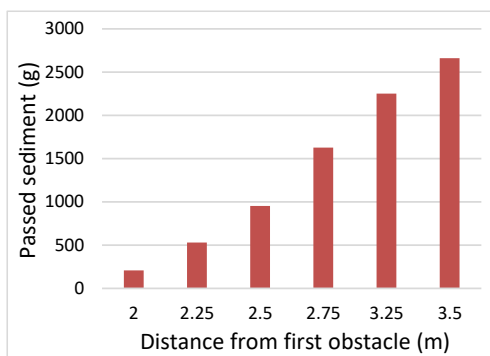


Figure 24. Amount of sediment behind second obstacle in terms of distance from first obstacle

not practically recognizable. Consequently, the optimum distance between the second and first obstacles was about 2.25 m.

6. CONCLUSION

This paper explores the effect of porosity and installation angle, thickness (dimension) and second layer of permeable obstacles on the density current control and trapping in the laboratory. Two types of groove and cavity obstacles with the groove width and cavity diameter equal to 3 mm were selected and built from the plexiglass sheets. An insoluble suspended polymer with the density of 1.135 g/l and average diameter of 1.15 mm was used to create the density current. The experiments were conducted at two different concentrations of 10 and 20%, five different porosities, four different angles, four different thicknesses and two obstacle layers:

- 1) The analysis of laboratory results showed that the optimum porosity for cavity and groove obstacles were 22 and 19%, respectively. However, an increasing porosity, the trapping up to the optimum porosity decreased and then increased.
- 2) In all tests, the trapping level of cavity obstacles was higher than the groove obstacles. The trapping level

of cavities obstacles at 10 and 20% concentrations were 0.13 and 0.14% higher than the groove obstacles, respectively.

- 3) The evaluation of different angles of obstacles relative to the direction perpendicular to the stream bed showed that by increasing the angle, the amount of trapping decreased. The reduction in the trapping level with the correlation coefficients of 0.995 and 0.981 in the groove obstacles was higher than the cavity ones.
- 4) The average flow velocity in the cavity obstacles was 3.62% higher than that in the groove obstacles.
- 5) For the increased thickness with 10% porosity and groove type, the passage of materials from the obstacle further increased. This was attributed to high flow velocity along with obstacle and the induced tensile force and its effect on the upstream inflow.
- 6) By creating the second layer of obstacle, the passage of materials from the obstacle in both groove and cavity obstacles increased, so that the amounts of 1.96% and 2.34% were recorded in the groove and cavity types, respectively. The reason for such increase was the effect of turbulent flow passing over the second obstacle. Therefore, higher the distance between the second and first obstacles resulted in improvement in trapping and sedimentation efficiencies. As such, the optimal distance from the second obstacle to the first one was obtained equal to 2.25 m. Beyond this distance, due to the effect of the turbulent flume inflow and injection of density current, the share of second obstacle was not noticeable. However, the effect of second layer on the overall trapping and sedimentation efficiencies was found to be positive. According to all obtained results, the cavity obstacles always outperformed the groove obstacles under similar conditions.

7. REFERENCES

1. Jawaduddin, M., Memon, S. A., Bheel, N., Ali, F., Ahmed, N., and Abro, A. W., "Synthetic Grey Water Treatment Through FeCl₃-Activated Carbon Obtained from Cotton Stalks and River Sand." *Civil Engineering Journal*, Vol. 5, No. 2, (2019), 340-348, doi: 10.28991/cej-2019-03091249.
2. Alavi, S. R., Lay, E. N., and Makhmal, Z. A., "A CFD study of industrial double-cyclone in HDPE drying process", *Emerging Science Journal*, Vol. 2, No. 1, (2018), 31-38, doi: 10.28991/esj-2018-01125.
3. Li, N., Sheng, G. P., Lu, Y. Z., Zeng, R. J. and Yu, H. Q., "Removal of antibiotic resistance genes from wastewater treatment plant effluent by coagulation", *Water Research*, Vol. 111, No. 1, (2017), 204-212, doi: 10.1016/j.watres.2017.01.010.
4. Massoudinejad, M., Hashempour, Y., and Mohammad, H. "Evaluation of Carbon Aerogel Manufacturing Process in Order to Desalination of Saline and Brackish Water in Laboratory

- Scale.”, *Civil Engineering Journal*, Vol. 4, No. 1, (2018), 212-220, doi: 10.28991/cej-030980.
5. Barahmand, N., and Shamsai, A., “Experimental and theoretical study of density jumps on smooth and rough beds, Lakes & Reservoirs” *Research and Management*, Vol. 15, No. 4, (2010) 285-306, doi: 10.1111/j.1440-1770.2010.00442.x.
 6. Hu, P., Cao, Z., Pender, G., and Tan, G., “Numerical modelling of turbidity currents in the Xiaolangdi reservoir, Yellow River, China”, *Journal of Hydrology*, Vol. 464, (2012), 41-53, doi: 10.1016/j.jhydrol.2012.06.032.
 7. Vladimirov, I.Y., Korchagin, N., and Savin, A., “Wave influence of a suspension-carrying current on an obstacle in the flow”, in *Doklady Earth Sciences*, Springer Science & Business Media, (2015), 286-293, doi: 10.1134/S1028334X15030162.
 8. Farizan, A., Yaghoubi, S., Firoozabadi, B., and Afshin, H., “Effect of an obstacle on the depositional behaviour of turbidity currents”, *Journal of Hydraulic Research*, Vol. 57, No. 1, (2019), 75-89, doi: 10.1080/00221686.2018.1459891.
 9. Chamoun, S., De Cesare, G., and Schleiss, A.J., “Managing reservoir sedimentation by venting turbidity currents: A review”, *International Journal of Sediment Research*, Vol. 31, No. 3, (2016), 195-204, doi: 10.1016/j.ijsrc.2016.06.001.
 10. Asghari Pari, S.A., Kashefipour, S.M., and Ghomeshi, M., “An experimental study to determine the obstacle height required for the control of subcritical and supercritical gravity currents”, *European Journal of Environmental and Civil Engineering*, Vol. 21, No. 9, (2017), 1080-1092, doi: 10.1080/19648189.2016.1144537.
 11. Yaghoubi, S., Afshin, H., Firoozabadi, B., and Farizan, A., “Experimental investigation of the effect of inlet concentration on the behavior of turbidity currents in the presence of two consecutive obstacles”, *Journal of Waterway, Port, Coastal, and Ocean Engineering*, Vol. 143, No. 2, (2016), 6018-6029, doi: 10.1061/(ASCE)WW.1943-5460.0000358.
 12. Keshtkar, MM. and Amiri, B., “Numerical simulation of radiative-conductive heat transfer in an enclosure with an isotherm obstacle”, *Heat Transfer Engineering*, Vol. 39, No. 1, (2018), 72-83, doi: 10.1080/01457632.2017.1280293.
 13. De Cesare, G., Oehy, C.D., and Schleiss, A.J., “Circulation in stratified lakes due to flood-induced turbidity currents”, *Journal of Environmental Engineering*, Vol. 132, No. 1, (2006), 1508-1517, doi: 10.1061/(ASCE)0733-9372(2006)132:11(1508).
 14. Asghari Pari, S. A., Habibagahi, G., Ghahramani, A., and Fakharian, K., “Improve the design process of pile foundations using construction control techniques.”, *International Journal of Geotechnical Engineering*, Vol. 1, No. 1, (2019), 1-8, doi: 10.1080/19386362.2019.1655622.
 15. Oehy, C.D., and Schleiss, A.J., “Control of turbidity currents in reservoirs by solid and permeable obstacles”, *Journal of Hydraulic Engineering*, Vol. 133, No. 6, (2007), 637-648, doi: 10.1061/(ASCE)0733-9429(2007)133:6(637).
 16. Kordnaej, A., Kalantary, F., Kordtabar, B. and Mola-Abasi, H., “Prediction of recompression index using GMDH-type neural network based on geotechnical soil properties”, *Soils and Foundations*, Vol. 55, No. 6, (2015), 1335-1345, doi: 10.1016/j.sandf.2015.10.001.
 17. Asghari Pari, S.A, Habibagahi, G., Ghahramani, A. and Fakharian, K., “Reliability-Based Calibration of Resistance Factors in LRFD Method for Driven Pile Foundations on Inshore Regions of Iran”, *International Journal of Civil Engineering*, Vol. 17, No. 12, (2019), 1859-1870, doi: 10.1007/s40999-019-00443-0.
 18. Samadi-koucheksaraee, A., Ahmadianfar, I., Bozorg-Haddad, O., and Asghari-pari, S. A., “Gradient evolution optimization algorithm to optimize reservoir operation systems”, *Water Resources Management*, Vol. 33, No. 2, (2019) 603-625, doi: 10.1007/s11269-018-2122-2.
 19. Marosi, M., Ghomeshi, M., and Sarkardeh, H., “Sedimentation control in the reservoirs by using an obstacle”, *Sadhana*, Vol. 40, No. 4, (2015), 1373-1383, doi: 10.1007/s12046-015-0333-2.
 20. Alves, M., Gaillard, F., Sparrow, M., Knoll, M., and Giraud, S., “Circulation patterns and transport of the Azores Front-Current system”, *Deep Sea Research Part II: Topical Studies in Oceanography*, Vol. 49, No. 19, (2002), 3983-4002, doi: 10.1016/S0967-0645(02)00138-8.
 21. Nogueira, W., Litvak, L., Edler, B., Ostermann, J., and Büchner, A., “Signal processing strategies for cochlear implants using current steering *EURASIP Journal on Advances in Signal Processing*, Vol. 1, (2009), 213-224, doi: 10.1155/2009/531213.
 22. Janocko, M., Cartigny, M., Nemeč, W., and Hansen, E., “Turbidity current hydraulics and sediment deposition in erodible sinuous channels: laboratory experiments and numerical simulations”, *Journal of Marine Petroleum Geology*, Vol. 41, (2013), 222-249, doi: 10.1016/j.marpetgeo.2012.08.012.
 23. McArthur, J. M., Sikdar, P. K., Nath, B., Grassineau, N., Marshall, J. D. and Banerjee, D. M., “Sedimentological control on Mn, and other trace elements, in groundwater of the Bengal Delta”, *Journal of Marine Petroleum Geology*, Vol. 46, No. 2, (2012), 669-676, doi: 10.1021/es202673n.
 24. Oshaghi, M. R., Afshin, H. and Firoozabadi, B., “Experimental investigation of the effect of obstacles on the behavior of turbidity currents”, *Canadian Journal of Civil Engineering*, Vol. 40, No. 4, (2013), 343-352, doi: 10.1139/cjce-2012-0429.
 25. Bogdanov, I. I., Mourzenko, V. V., Thovert, J. F. and Adler, P. M., “Effective permeability of fractured porous media in steady state flow”, *Water Resources Research*, Vol. 39, No. 1, (2003), 13-24, doi: 10.1029/2001WR000756.
 26. Abhari, M.N., Iranshahi, M., Ghodsian, M., and Firoozabadi, B., “Experimental study of obstacle effect on sediment transport of turbidity currents”, *Journal of Hydraulic Research*, Vol. 56, No. 5, (2018), 618-629, doi: 10.1080/00221686.2017.1397778.
 27. Wilson, R. I. and Friedrich, H., “Coupling of Ultrasonic and Photometric Techniques for Synchronous Measurements of Unconfined Turbidity Currents”, *Water*, Vol. 10, No. 9, (2018), 1246-1258, doi: 10.3390/w10091246.
 28. Tokyay, T., Constantinescu, G., and Meiburg, E., “Lock-exchange gravity currents with a high volume of release propagating over a periodic array of obstacles”, *Journal of Fluid Mechanics*, Vol. 672, (2011), 570-605, doi: 10.1017/S0022112010006312.
 29. Tokyay, T., Constantinescu, G., Gonzalez-Juez, E., and Meiburg, E., “Gravity currents propagating over periodic arrays of blunt obstacles: Effect of the obstacle size”, *Journal of Fluids and Structures*, Vol. 27, No. 6, (2011), 798-806, doi: 10.1016/j.jfluidstructs.2011.01.006.
 30. Nasr-Azadani, M., and Meiburg, E., “Turbidity currents interacting with three-dimensional seafloor topography”, *Journal of Fluid Mechanics*, Vol. 745, (2014), 409-443, doi: 10.1017/jfm.2014.47.

Persian Abstract

چکیده

در این پژوهش، اثر تخلخل و زاویه‌ی نصب، ضخامت (بعد) و لایه دوم موانع نفوذپذیر بر کنترل و تله‌اندازی جریان غلیظ در آزمایشگاه بررسی شده است. برای این منظور، از یک پلیمر نامحلول و معلق و موانع از صفحات پلاکسی گلاس انتخاب شدند که از دو نوع شیباری و حفره‌ای استفاده شد. آزمایش‌ها با دو غلظت متفاوت، پنج تخلخل گوناگون، چهار زاویه‌ی مختلف، چهار ضخامت متفاوت و با دو لایه مانع انجام شدند. نتیجه‌ها نشان دادند که با افزایش تخلخل، میزان تله‌اندازی تا تخلخل بهینه روند کاهشی و سپس افزایشی دارد. بر این اساس، تخلخل بهینه برای موانع حفره‌ای و موانع شیباری به ترتیب ۲۲ و ۱۹ درصد به دست آمد. در همه‌ی آزمایش‌ها، تله‌اندازی حفره‌ای، با ۰/۱۳ و ۰/۱۴ درصد به ترتیب در غلظت‌های ۱۰ و ۲۰ درصد، بیشتر از شیباری بود. علاوه بر این، با افزایش زاویه، مقدار تله‌اندازی کاهش یافت و مقدار آن در شیباری نسبت به حفره‌ای به ترتیب با ضریب همبستگی‌هایی برابر ۰/۹۹۵ و ۰/۹۸۱، بیشتر مشاهده شد. اثر عمده موانع، کاهش سرعت و ایجاد کندی جریان تشخیص داده شد که متوسط سرعت در حفره‌ای ۳/۶۲ درصد بیشتر از شیباری به دست آمد. به ازای افزایش ضخامت با تخلخل ۱۰ درصد و نوع شیباری روند عبور مواد از مانع بیشتر شد. با ایجاد لایه دوم مانع عبور موارد از مانع هم در شیباری و هم در حفره‌ای روند افزایشی پیدا کرد و فاصله بهینه مانع دوم از اول معادل ۲/۲۵ متر به دست آمد.
